Electronic Supplementary Material (ESI) for Analytical Methods.

Electronic Supplementary Material (ESI)

A novel NBD-based fluorescent turn-on probe for detection of phosgene in solution and the gas phase

Lei Yang,[a] Zhiwei Sun,*[a] Zan Li,[a] Xiaojian Kong,[c] Feng Wang,[a] Xuefang Liu,[a] Jingpu Tang,[a] Meiling Ping[a] and Jinmao You[ab]

[a] *Key Laboratory of Life-Organic Analysis of Shandong Province, Qufu Normal University, Qufu 273165, China*

[b] *Key Laboratory of Tibetan Medicine Research, Qinghai Key Laboratory of Qinghai-Tibet Plateau Biological Resources, Northwest Institute of Plateau Biology, Chinese Academy of Science, Xining 810001, China*

[c] *School of Chemical New Material Engineering, Shandong Polytechnic College, Jining, 272027, China*

*Corresponding author.

Z. Sun, zhiweisun@qfnu.edu.cn, sunzhiw@126.com

Table of Contents

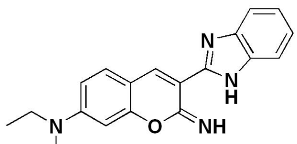

IC-phos

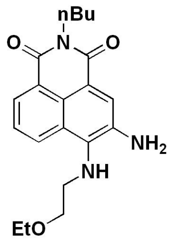

Phos-2

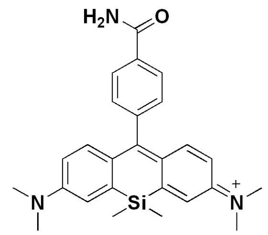

SiR-amide

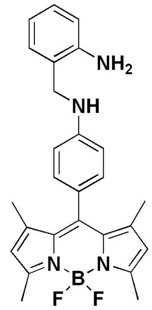

BOD-SYR

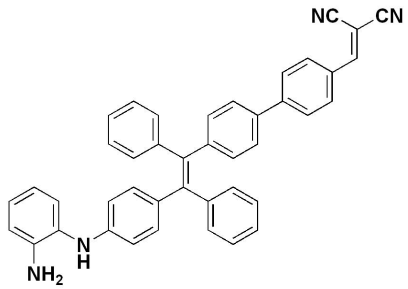

OPD-TPE-Py-2CN

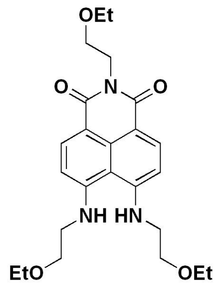

Phos-1

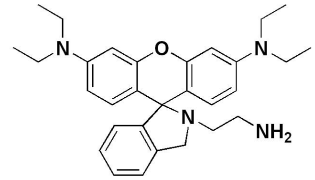

dRB-EDA

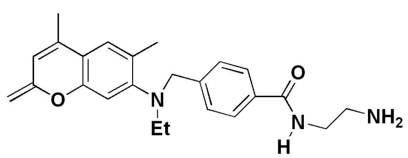

Coumarins 1

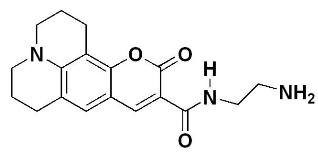

Coumarins 2

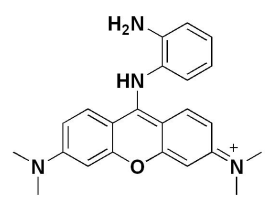

PY-OPD

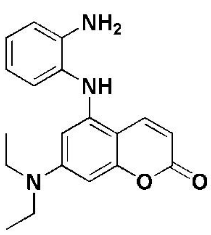

o-Pac

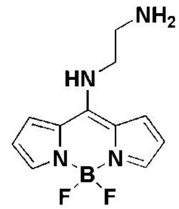

8-EDAB

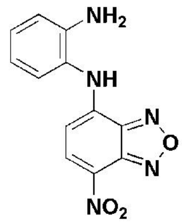

NBD-OPD

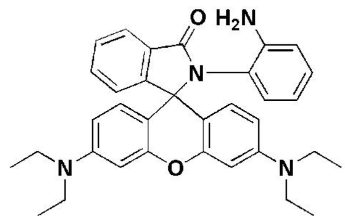

RB-OPD

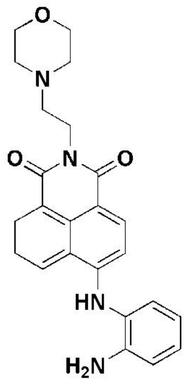

NAP-OPD

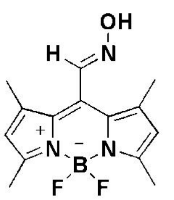

1-oxime

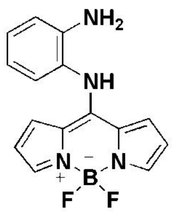

o-Pab

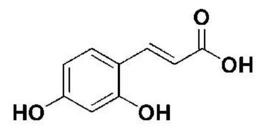

Kundu's <u>1</u>

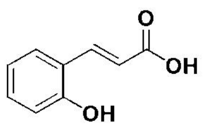

Kundu's <u>2</u>

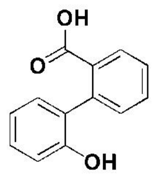

Kundu's <u>3</u>

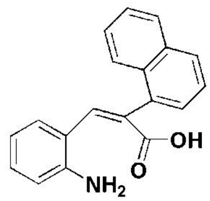

Kundu's <u>4</u>

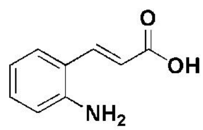

Kundu's <u>5</u>

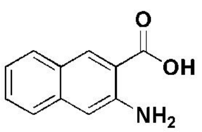

Kundu's <u>6</u>

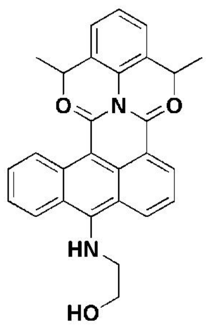

Ac-Phos

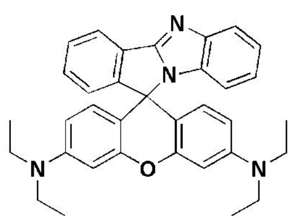

Sensor 1

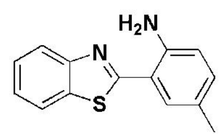

Chen's Probe 1

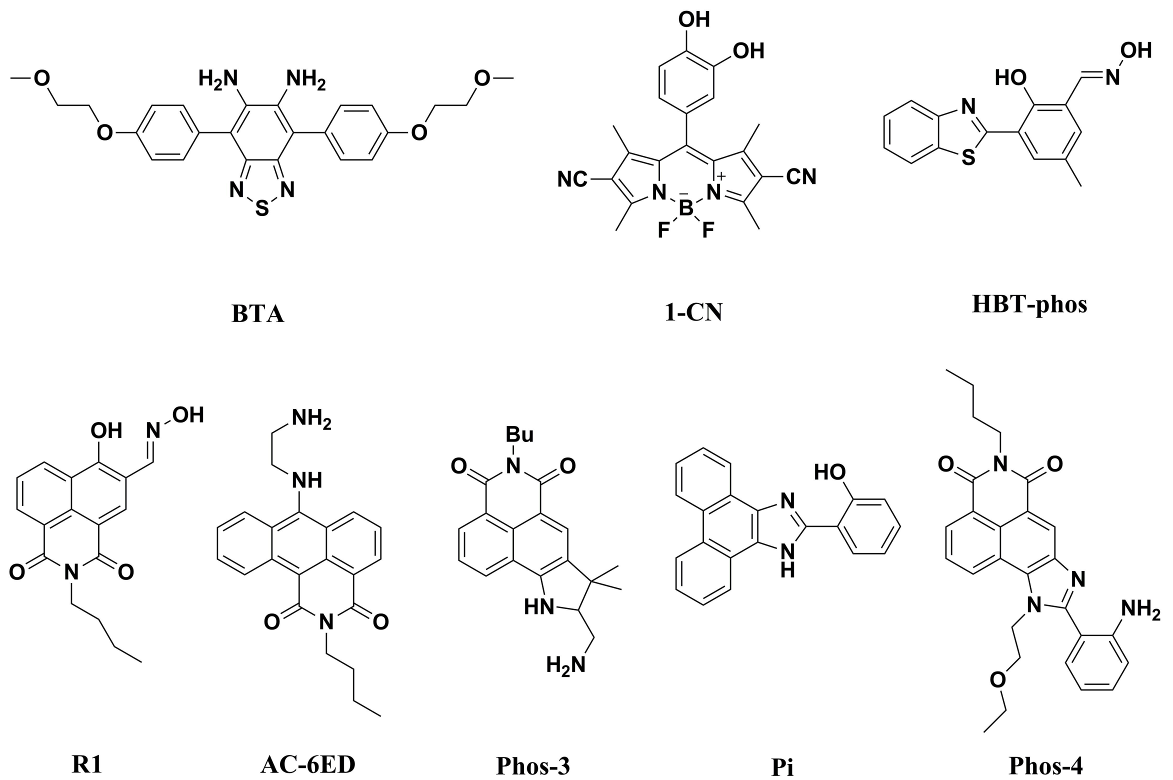

Fig. S1. Structures of probes recently reported for phosgene detection.

Table S1. Comparisons of recently reported strategies for phosgene detection.

Name and Literature	Mechanism	Ratiometric Or Turn-on	Fluorophore	$\lambda_{ex}/\lambda_{em}$ (nm)	Detection limit	Response time	References
IC-phos	ICT	Ratiometric	3-benzimidazole iminocoumarin	λ_{ex}=440nm λ_{em}=482/550 nm	27 nM (Phosgene)	2 min	1
Phos-2	ESIPT	Turn-on	Peridiamine of naphthalimide	λ_{ex}=400nm λ_{em}=468nm	0.2 nM (Triphosgene)	30 s	2
SiR-amide	Conversion of amide to nitrile	Turn-on	Si-rhodamine	λ_{ex}=653nm λ_{em}=679nm	8.9 nM (Triphosgene)	4 min	3
BOD-SYR	Block PET	Turn-on	BODIPY	λ_{ex}=460nm λ_{em}=511nm	179 nM (Triphosgene)	10 s	4
OPD-TPE-Py -2CN	AIE	Turn-on	Tetraphenylethene (TPE)	λ_{ex}=365nm λ_{em}=475nm	1.87 ppm (Phosgene)	2 min	5
Phos-1	ICT	Ratiometric	4,5-diamino-1,8-naphthalimide	λ_{ex}=410nm λ_{em}=511/442nm	1.3 nM (Triphosgene)	20 min	6
dRB-EDA	opening of the spiro-(deoxy) lactam	Turn-on	Rhodamine	λ_{ex}=560nm λ_{em}=590nm	50 nM (Triphosgene)	—	7
Coumarins 1 and 2	FRET	Ratiometric	Coumarin	λ_{ex}=343/435nm λ_{em}=425/468nm	50 μM (Triphosgene)	within seconds	8
PY-OPD	Block PET	Turn-on	Pyronin	λ_{ex}=580nm λ_{em}=593nm	20 nM (Triphosgene)	2 min	9
o-Pac	Block PET	Turn-on	7-(diethylamino)-coumarin	λ_{ex}=368nm λ_{em}=446nm	3 nM (Triphosgene)	0.5 min	10

8-EDAB	ICT	Ratiometric	BODIPY	λ_{ex}=390/465nm λ_{em}=445/512nm	0.12 nM (Phosgene)	1.5 s	11
NBD-OPD	Block PET	Turn-on	7-nitrobenzo[c][1,2,5]oxadiazole	λ_{ex}=270nm λ_{em}=308nm	0.7 ppb (Triphosgene)	2 min	12
RB-OPD	Block PET	Turn-on	Rhodamine	λ_{ex}=530nm λ_{em}=575nm	2.8 ppb (Triphosgene)	1 min	12
NAP-OPD	Block PET	Turn-on	1,8-naphthalimide	λ_{ex}=340nm λ_{em}=480nm	2.8 ppb (Triphosgene)	3 min	12
1-oxime	Dehydration of oxime to nitrile	Turn-on	BODIPY	λ_{ex}=530nm λ_{em}=570nm	0.09 ppb (Triphosgene)	10 s	13
o-Pab	Block PET	Turn-on	BODIPY	λ_{ex}=450nm λ_{em}=530nm	2.7 nM (Triphosgene)	15 s	14
Kundu's 1	Intramolecular cyclization	Turn-on	7-hydroxy coumarin	λ_{ex}=330nm λ_{em}=382nm	9 nM (Phosgene)	—	15
Kundu's 2	Intramolecular cyclization	Turn-on	Coumarin	λ_{ex}=315nm λ_{em}=378nm	18 nM (Phosgene)	—	15
Kundu's 3	Intramolecular cyclization	Turn-on	6H-benzo[c] chromen-6-one	λ_{ex}=330nm λ_{em}=395nm	14 nM (Phosgene)	—	15
Kundu's 4	Intramolecular cyclization	Turn-on	3-(naphthalen-1-yl) quinolin-2(1H)-one	λ_{ex}=380nm λ_{em}=428nm	2 nM (Phosgene)	—	15
Kundu's 5	Intramolecular cyclization	Turn-on	Quinolin-2(1H)-one	λ_{ex}=380nm λ_{em}=452nm	1 nM (Phosgene)	—	15
Kundu's 6	Intramolecular cyclization	Turn-on	Naphtho[2,3-b] azet-2(1H)-one	λ_{ex}=380nm λ_{em}=430nm	6 nM (Phosgene)	—	15

Ac-Phos	Inhibit ICT	Ratiometric	Anthracene carboxyimide	λ_{ex}=434/502nm λ_{em}=482/615 nm	2.3 nM (Phosgene)	5 min	16
Sensor 1	Spirocyclic ring -open reaction	Turn-on	Benzimidazole -fused rhodamine	λ_{ex}=530nm λ_{em}=578nm	3.2 ppb (Triphosgene)	2 min	17
Chen's Probe 1	ESIPT	Ratiometric	2-(2-aminophenyl) benzothiazole	λ_{ex}=375nm λ_{em}=445/495nm	0.14 ppm (Phosgene)	5 min	18
BTA	ICT	Turn-on	Benzothiadiazole	λ_{ex}=380nm λ_{em}=508nm	20 nM (Phosgene)	20 min	19
1-CN	Block PET	Turn-on	BODIPY	λ_{ex}=480nm λ_{em}=516nm	24 pM (Phosgene)	within 3 s	20
HBT-phos	ESIPT	Turn-on	2-(2'-hydroxyphenyl)benzothiazole	λ_{ex}=438nm λ_{em}=474nm	0.48 nM (Phosgene)	20 min	21
R1	ESIPT	Ratiometric	3-oxime-4-hydroxy-1,8-naphthalic-n-butylamide	λ_{ex}=382nm λ_{em}=495/577nm	0.087 ppm (Phosgene)	1.43 s	22
AC-6ED	ICT	Ratiometric	Anthracene carboximide	λ_{ex}=470nm λ_{em}=520/610nm	0.09 nM (Phosgene)	Within 20 s	23
Phos-3	ICT	Ratiometric	Peridiamine of naphthalimide	λ_{ex}=400nm λ_{em}=488/548nm	0.3 nM (Phosgene)	60 s	24
Pi	ESIPT	Ratiometric	2-(1H-imidazol-2-yl) phenol	λ_{ex}=335nm λ_{em}=393/469nm	0.14 ppm (Phosgene)	30 s	25
Phos-4	ICT	Turn-on	1,8-naphthalimide	λ_{ex}=390nm λ_{em}=422/526nm	3.2 nM (Phosgene)	within 10 s	26
Probe 1	Block PET	Turn-on	7-nitro-2,1,3 -benzoxadiazole	λ_{ex}=460nm λ_{em}=525nm	1.2 nM (Triphosgene)	within 20 s	This work

"—" Not mentioned.

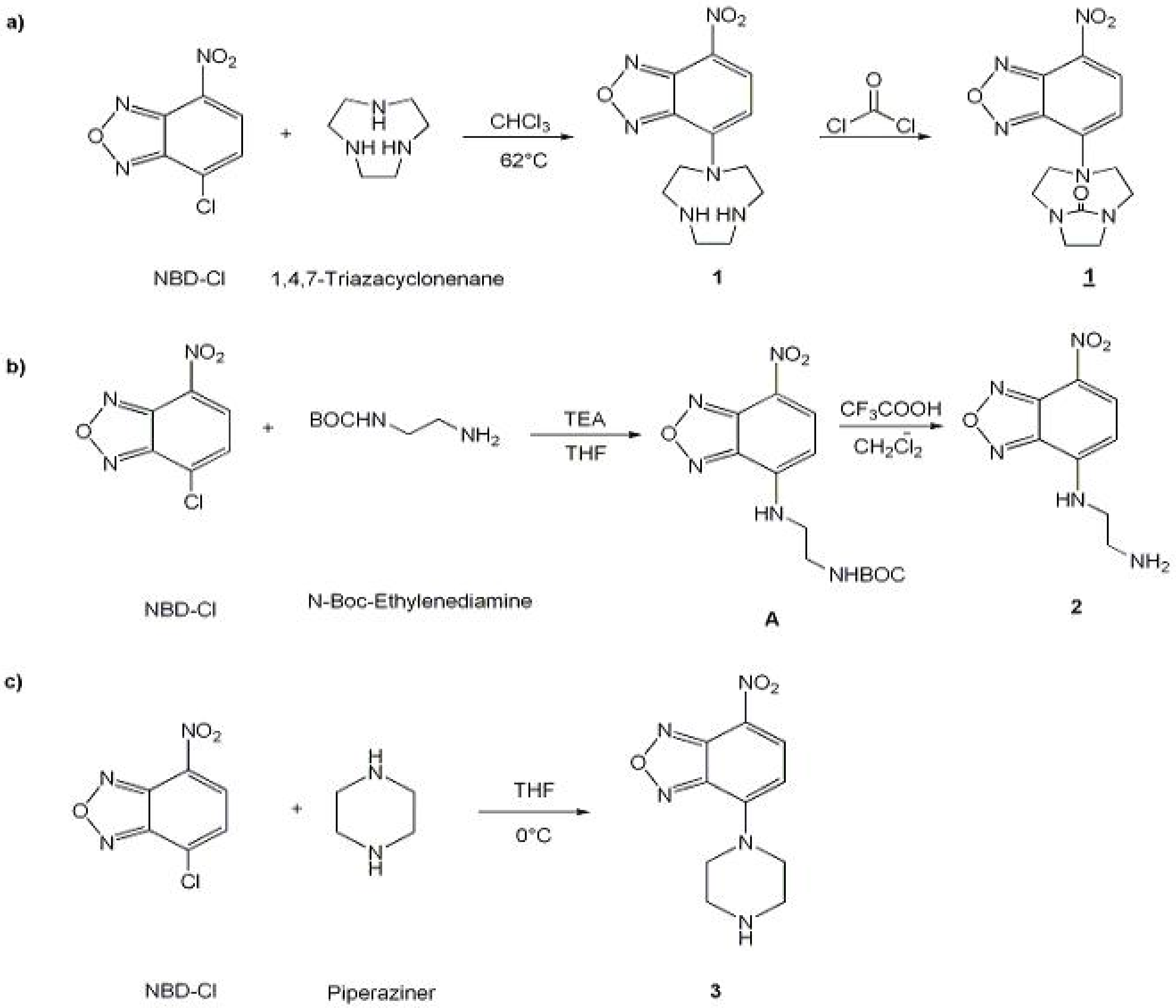

Fig. S2. Synthetic routes of probe 1(a), 2(b) and 3(c).

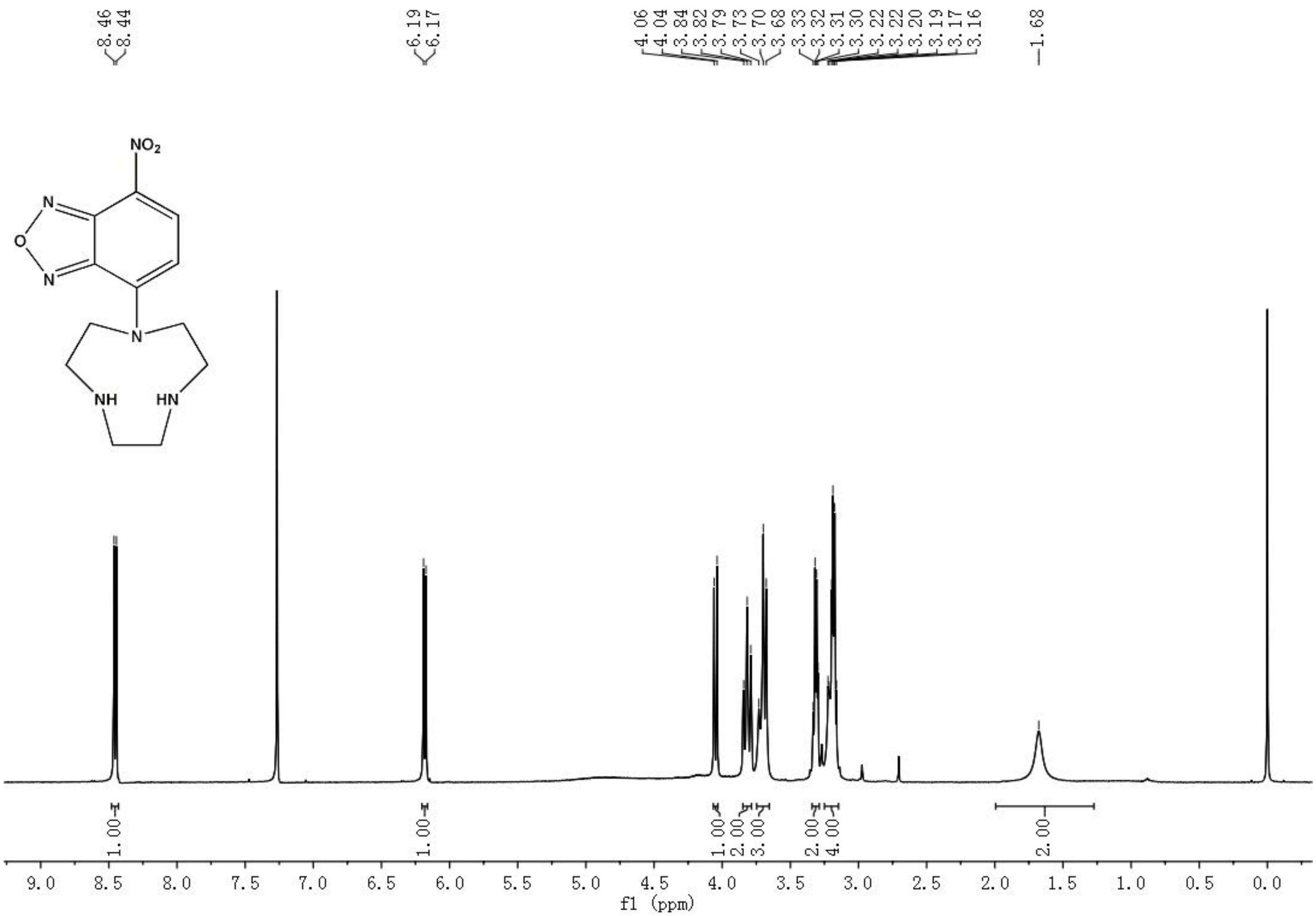

Fig. S3. ^{1}H NMR spectrum of probe **1** in $CDCl_3$ (500 MHZ).

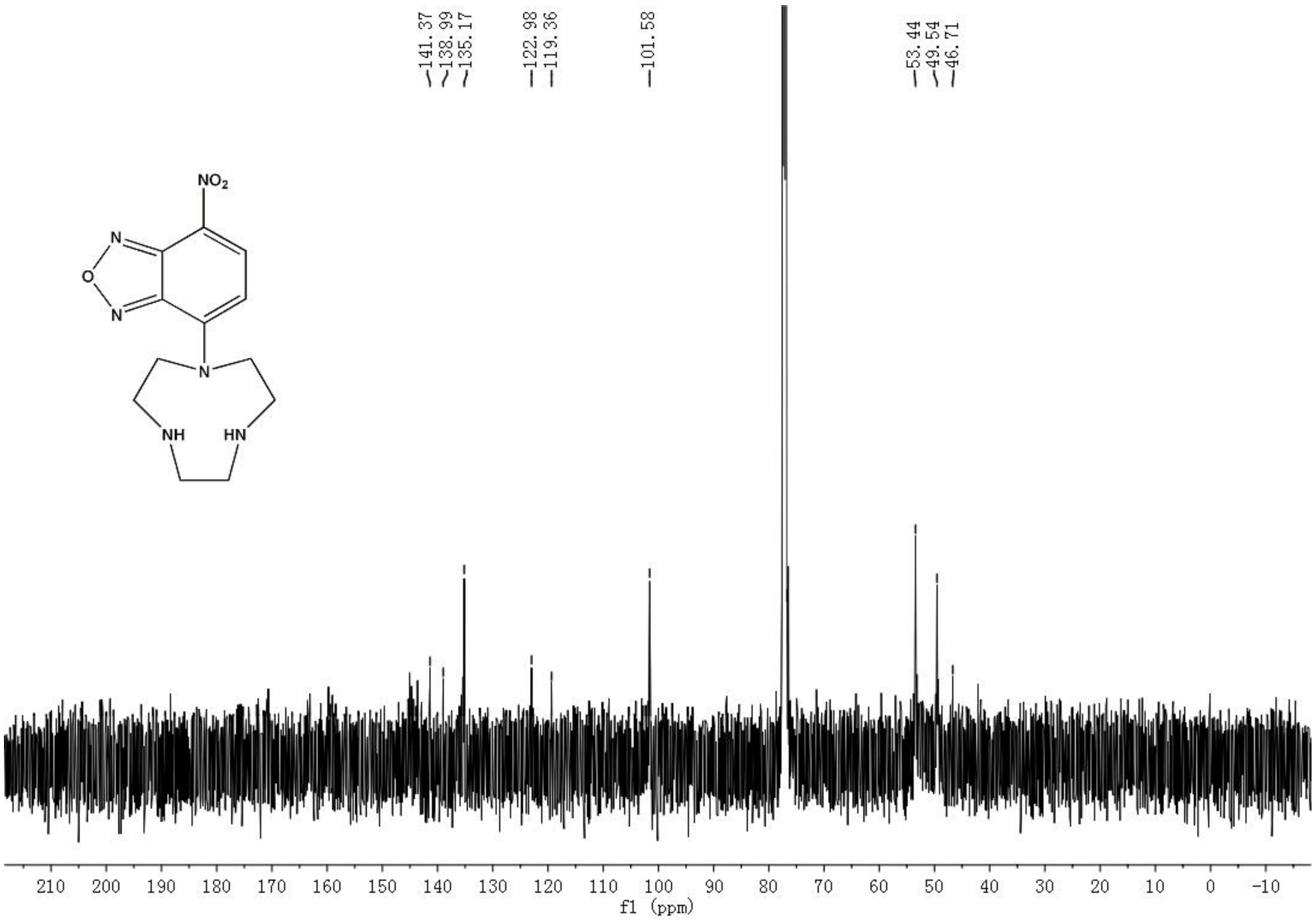

Fig. S4. ^{13}C NMR spectrum of probe **1** in $CDCl_3$ (125 MHZ).

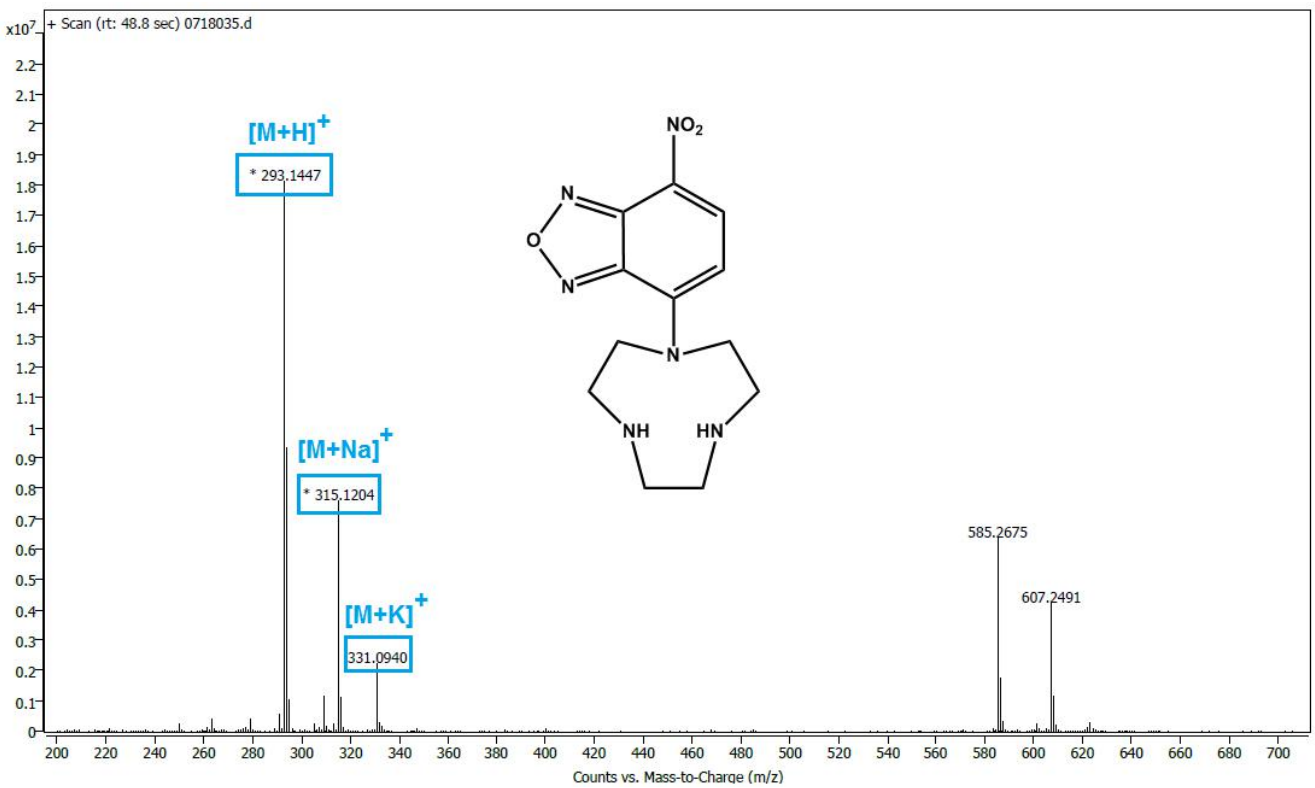

Fig. S5. ESI-HRMS spectrum of probe **1**.

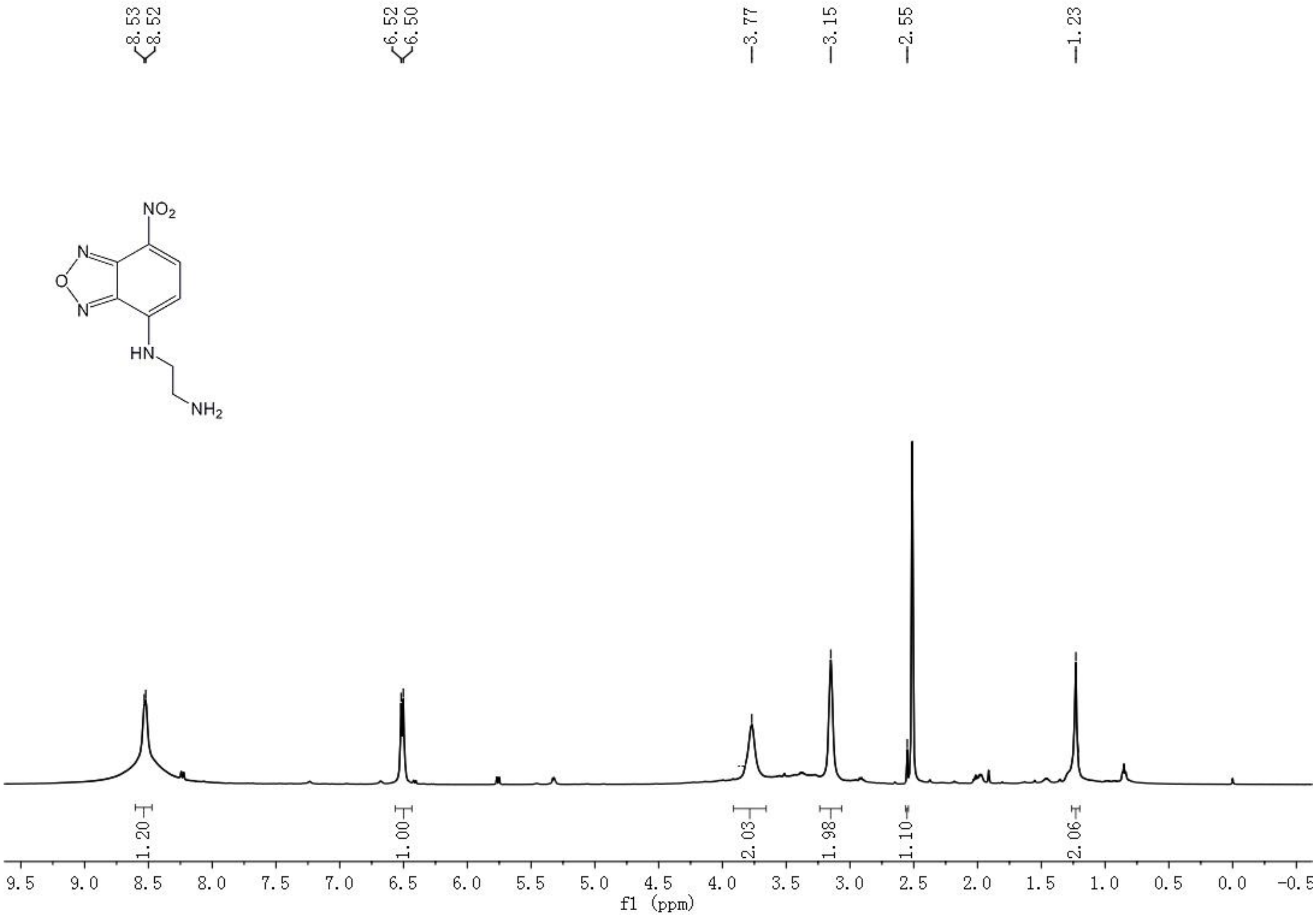

Fig. S6. ^{1}H NMR spectrum of probe **2** in DMSO (500 MHZ).

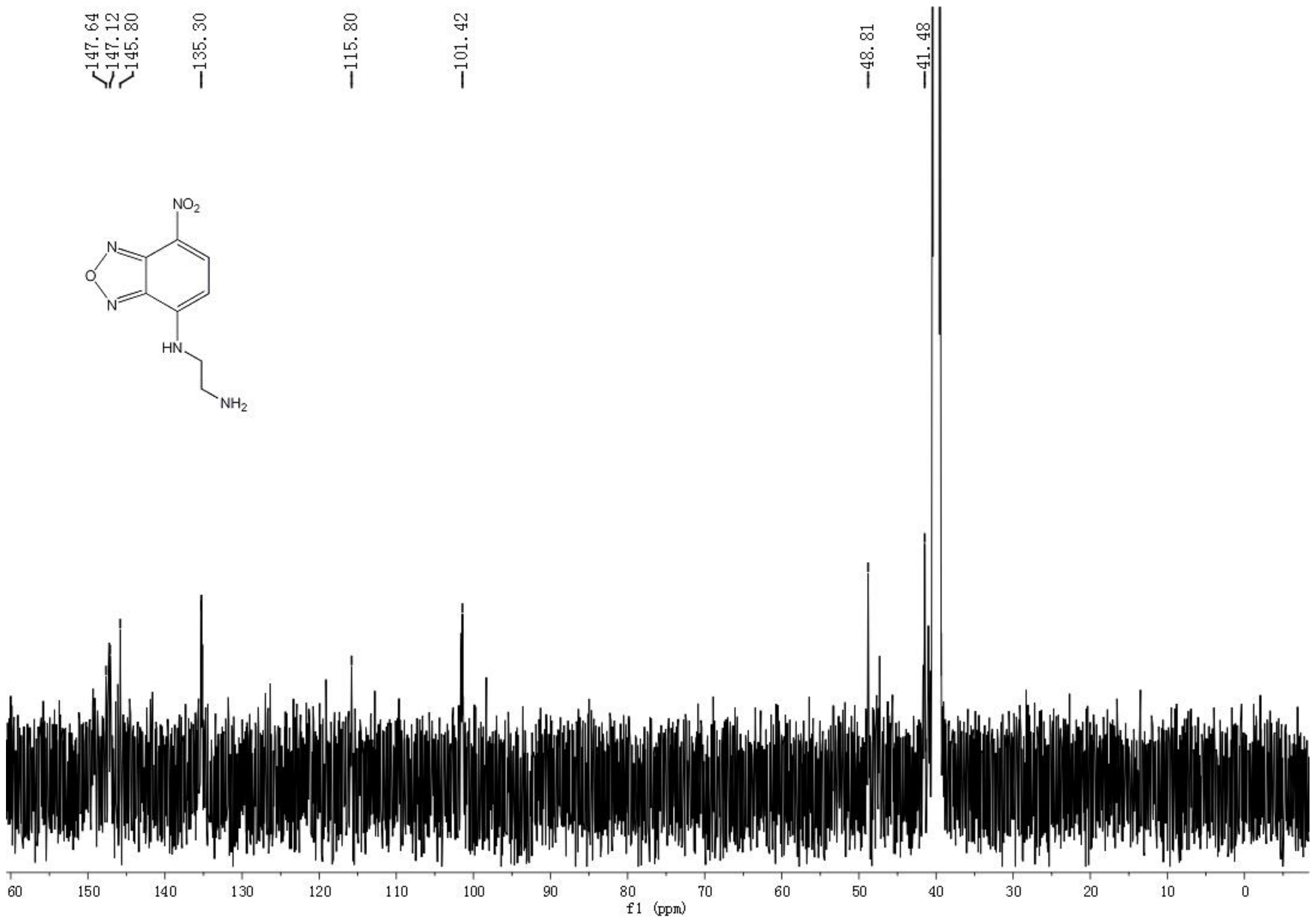

Fig. S7. ^{13}C NMR spectrum of probe **2** in DMSO (125 MHZ).

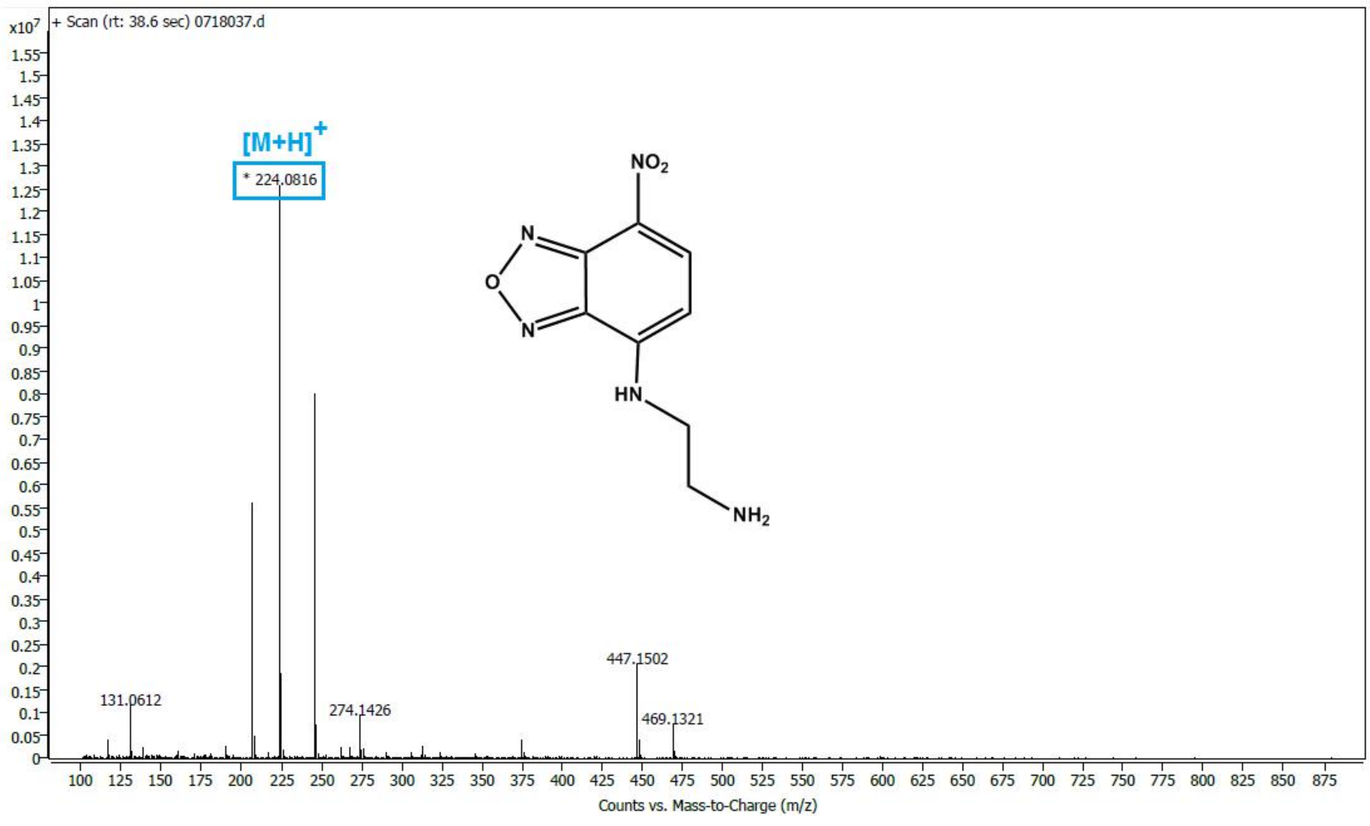

Fig. S8. ESI-HRMS spectrum of probe **2**.

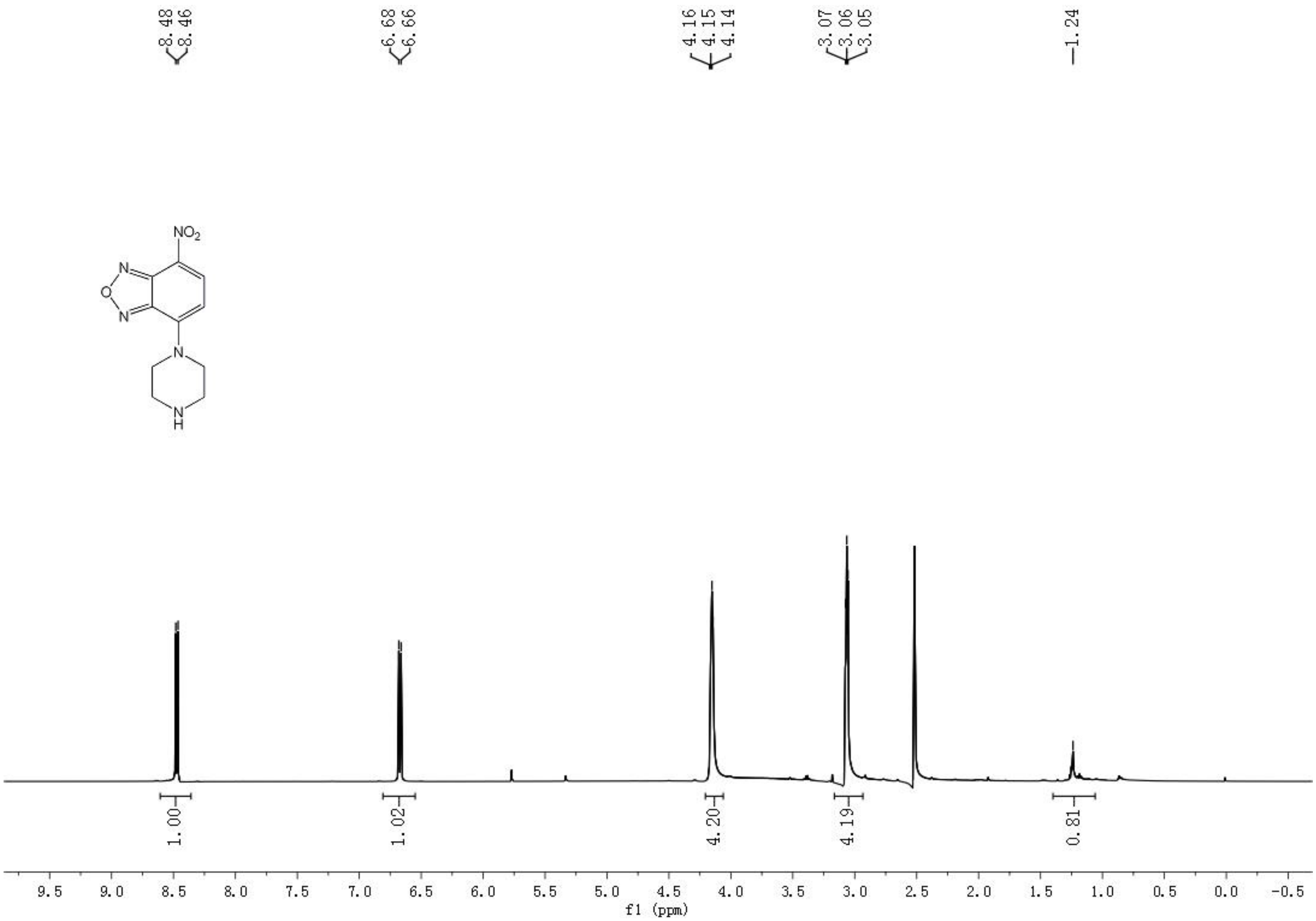

Fig. S9. ^{1}H NMR spectrum of probe **3** in DMSO (500 MHZ)

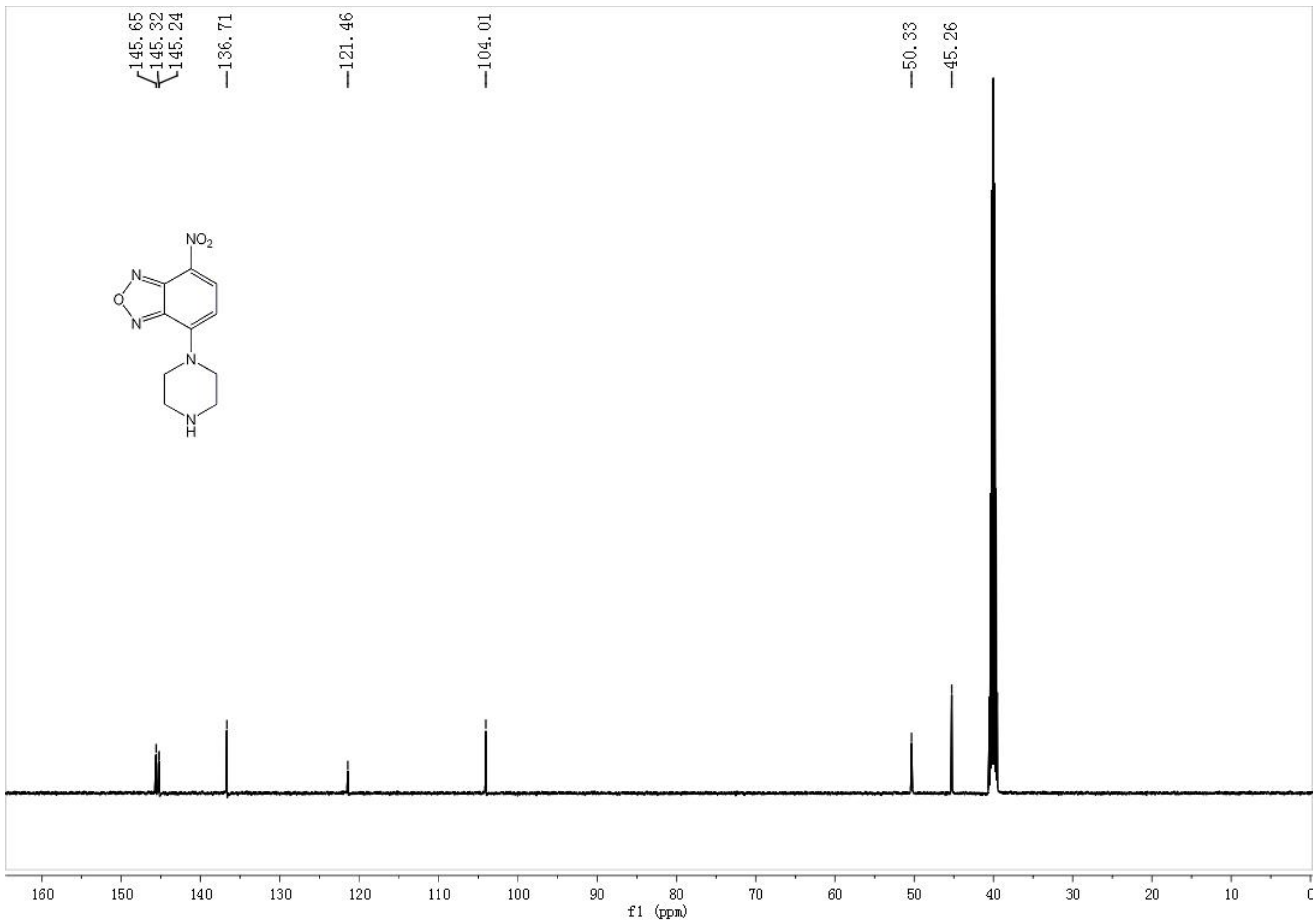

Fig. S10. ^{13}C NMR spectrum of probe **3** in DMSO (125 MHZ).

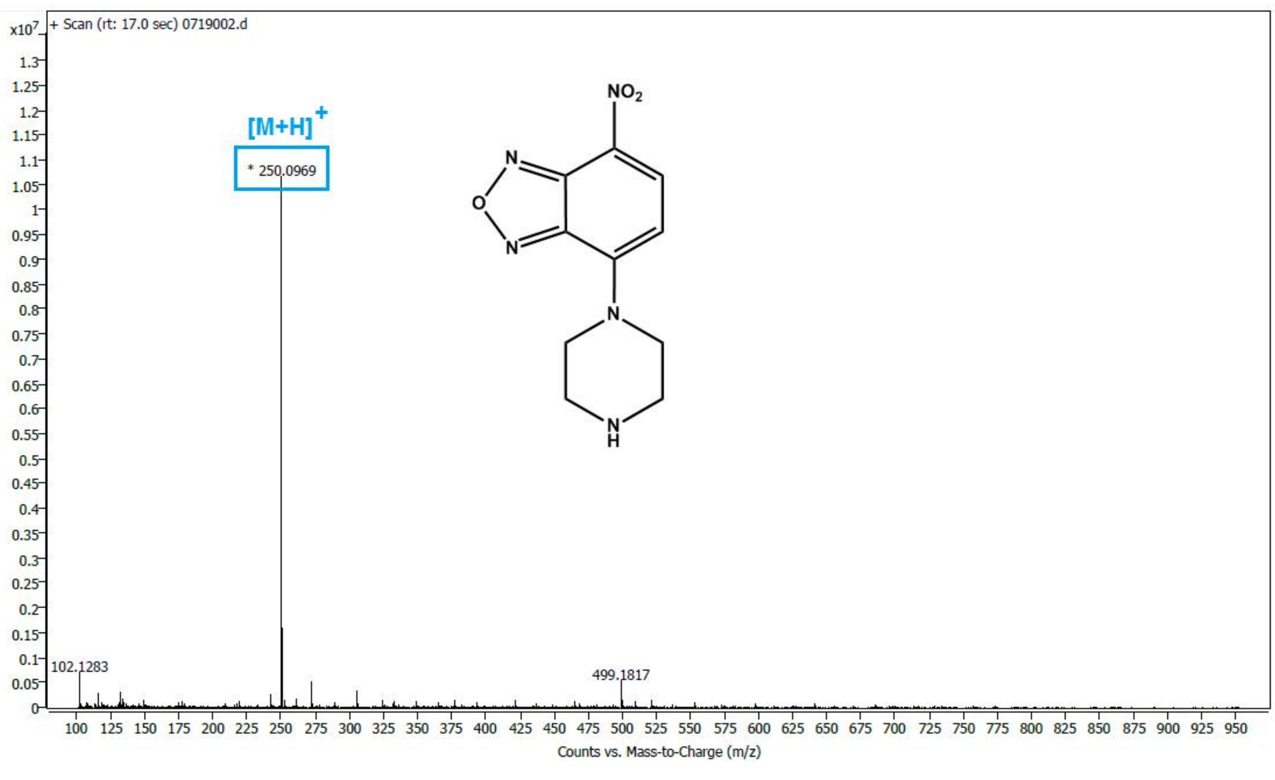

Fig. S11. ESI-HRMS spectrum of probe **3**.

Determination of the detection limit.

The detection limit for phosgene was calculated by the fluorescence titration experiments according to the reported method. A good linear relationship between the fluorescence intensity at 525 nm and triphosgene concentration (0 μM-4 μM) could be obtained (R^2=0.9995). The value obtained for the triphosgene was calculated as 1.2 nM by the equation of **Detection limit = 3σ/k** (Where **σ** is the standard deviation of the blank sample (measured 10 times) and **k** is the slope of the linear regression equation.). **σ**= 0.0386, **k** = 98.3379.

(a)

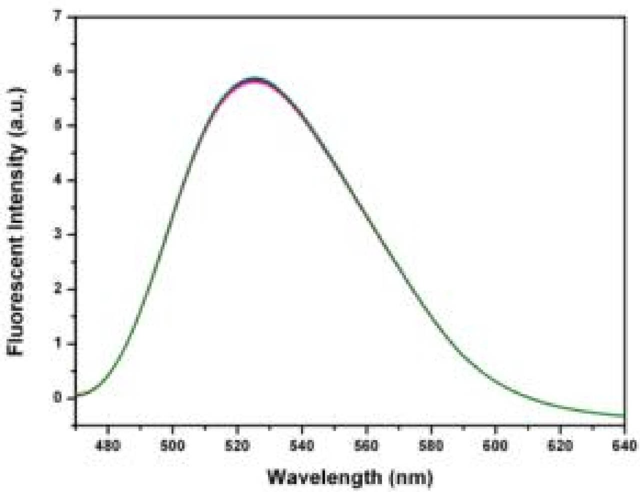

(b)

Blank Sample	F_{525}
1	5.87
2	5.83
3	5.87
4	5.87
5	5.84
6	5.86
7	5.84
8	5.84
9	5.81
10	5.96
σ	**3.86×10^{-2}**

Fig. S12. (a) Overlapped fluorescence spectra of 10 μM probe **1** in CH_3CN, λ_{ex} = 460 nm, slits: 5/5 nm; (b) Standard deviation (**σ**) of blank measurement.

(a)

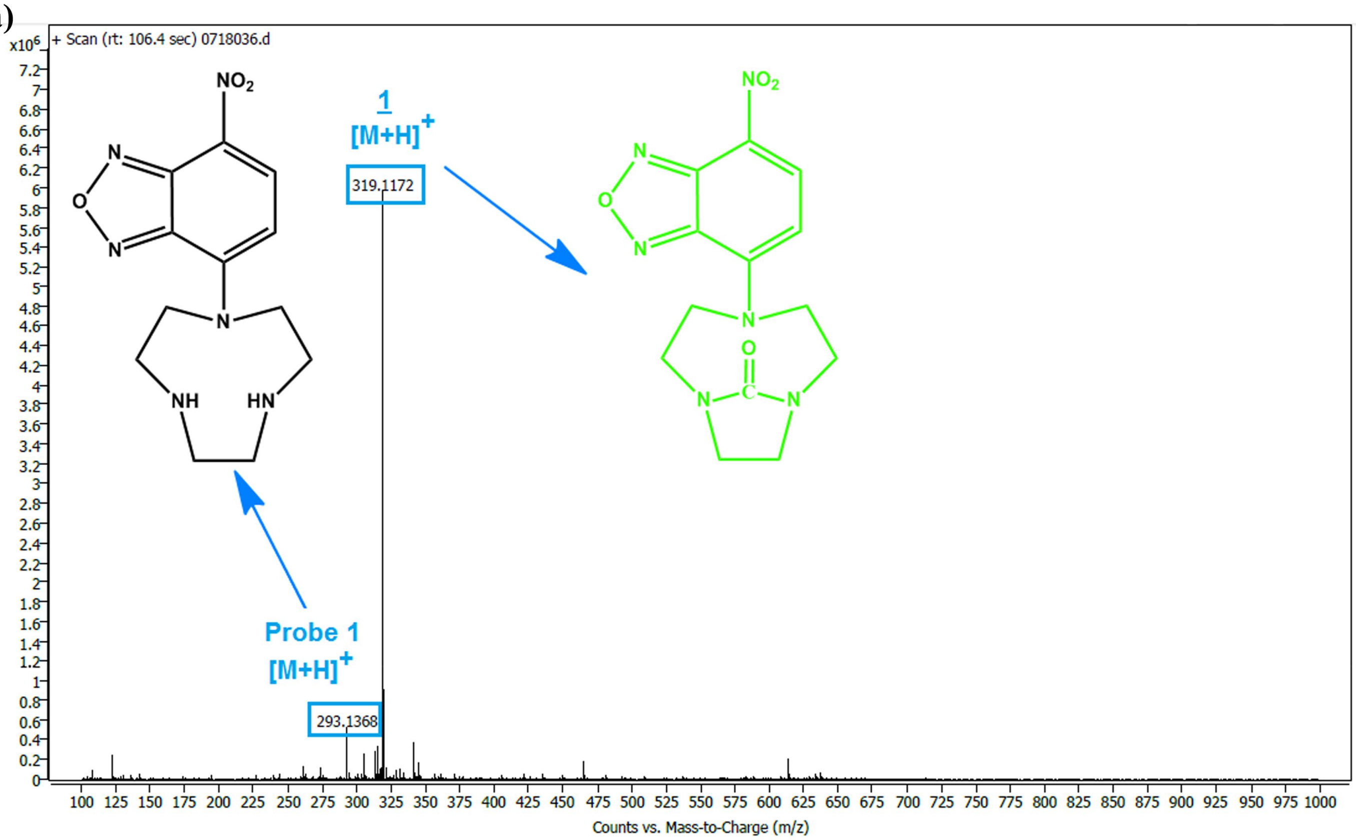

(b)

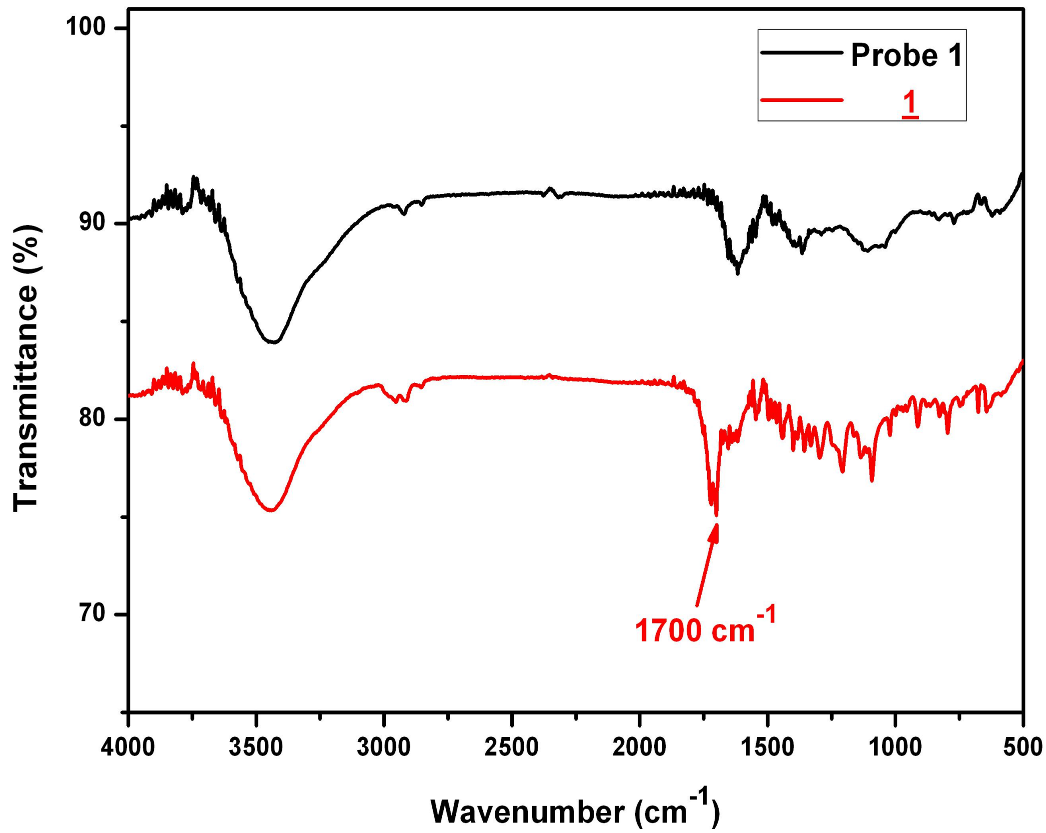

Fig. S13. ESI-HRMS(a) and IR(b) spectra of probe **1** and **1**.

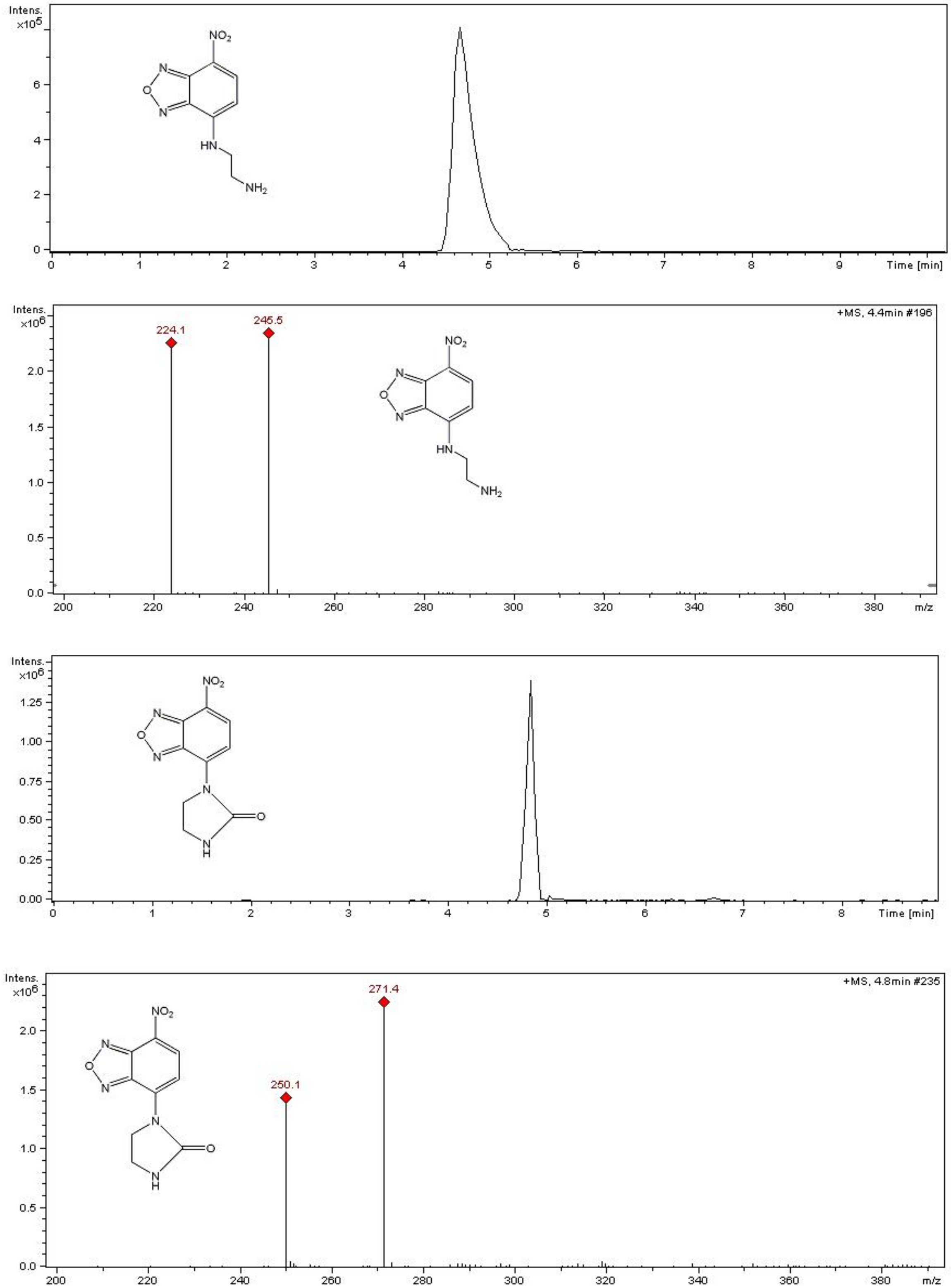

Fig. S14. HPLC-ESI-MS analysis of probe **2** before and after adding phosgene.

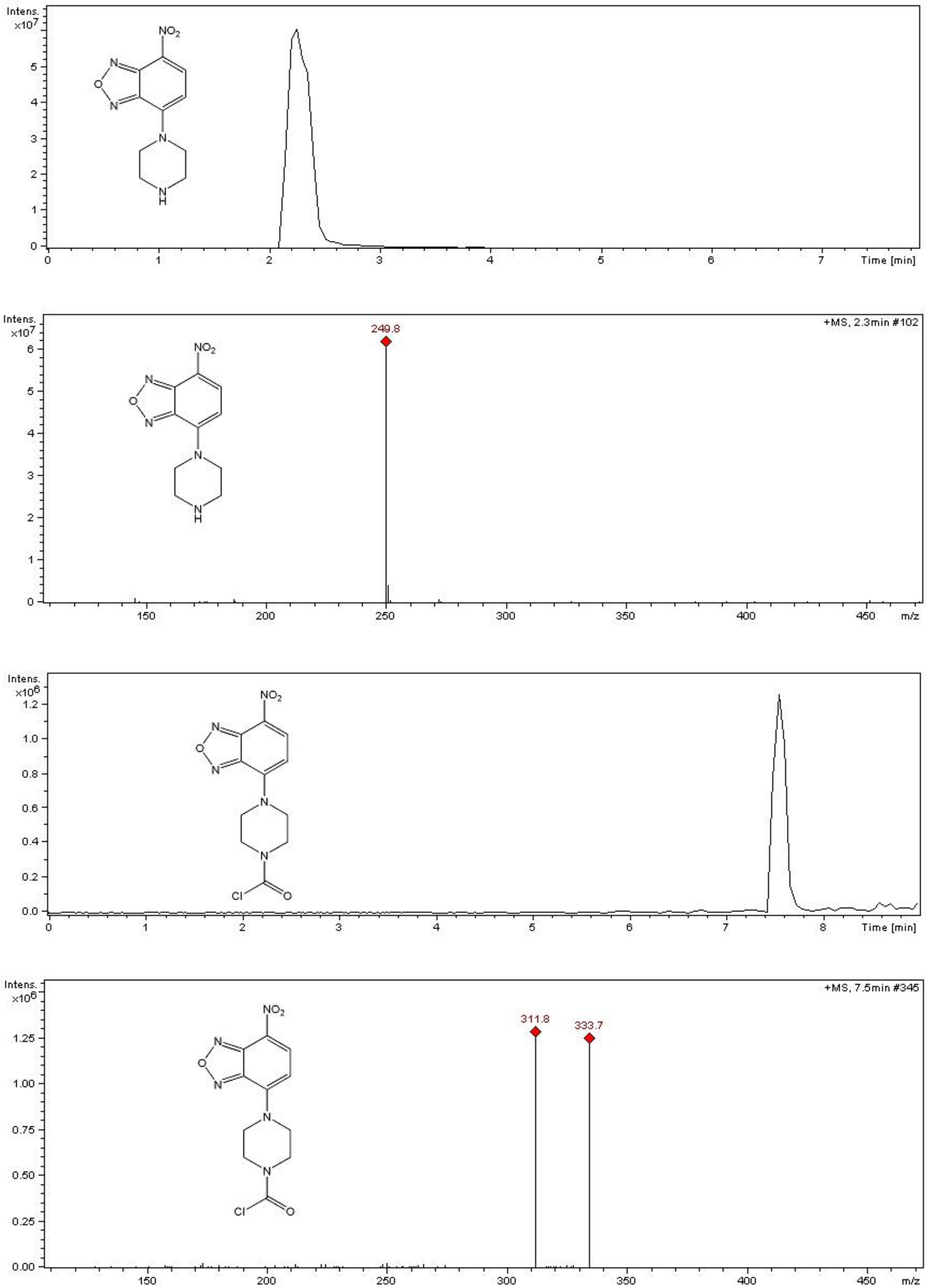

Fig. S15. HPLC-ESI-MS analysis of probe **3** before and after adding phosgene.

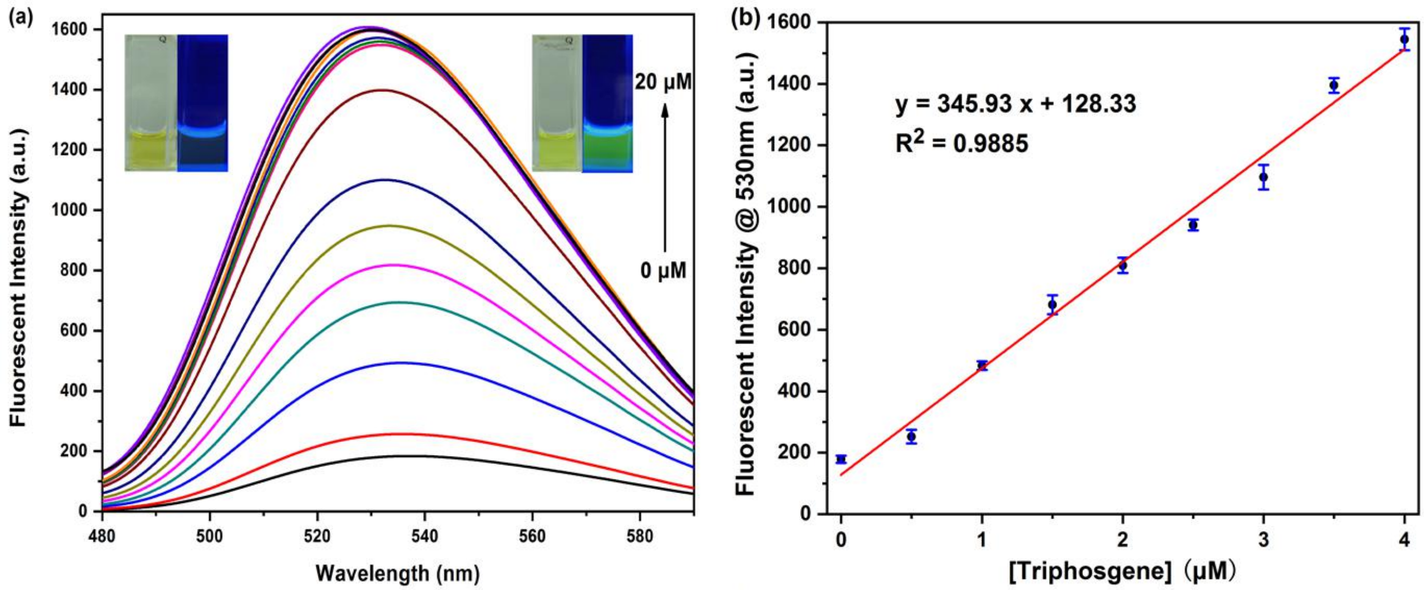

(c)

Blank Sample	F_{530}
1	172.7
2	167.8
3	168.5
4	169.2
5	169.8
6	170.4
7	170.7
8	171.1
9	171.8
10	172.2
σ	**2.32**

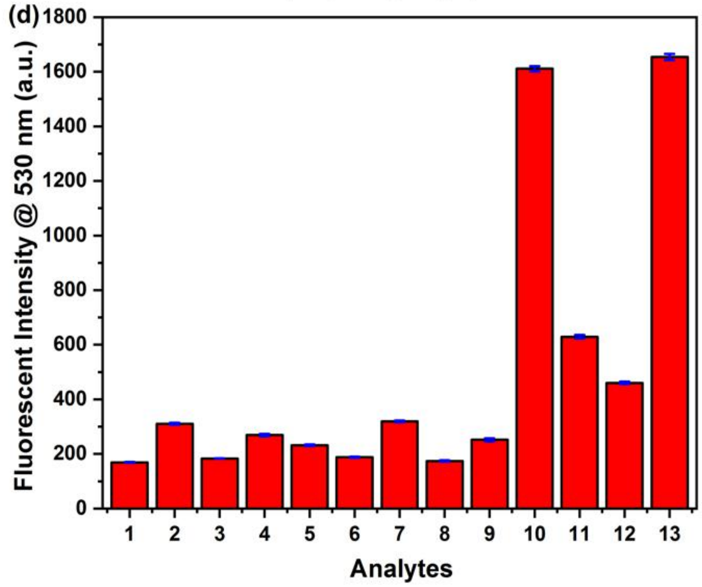

Fig. S16. (a) fluorescence spectra of Probe **2** (10 μM) in CH_3CN upon addition of an increasing amount of triphosgene (0−20 μM). (Inset) The color and fluorescence images of Probe **2** in the absence/ presence of triphosgene (λ_{ex} = 460 nm, slits: 10/10 nm). (b) The linear relationship between the fluorescence intensity at 530 nm and triphosgene concentration (0-4 μM) in CH_3CN; (c) Standard deviation (σ) of blank measurement from Fig. S16a; (d) fluorescent intensity at 530 nm of Probe **2** (10 μM) after the additions of analytes (30 μM) (1) Blank, (2) HCHO, (3) NO, (4) HCl, (5) $POCl_3$, (6) CH_3COCl, (7) $CH_2ClCOCl$, (8) $(COCl)_2$, (9) TsCl, (10) DCNP, (11) DCP, (12) $SOCl_2$, (13) Triphosgene (λ_{ex} = 460 nm, slits: 10/10 nm).

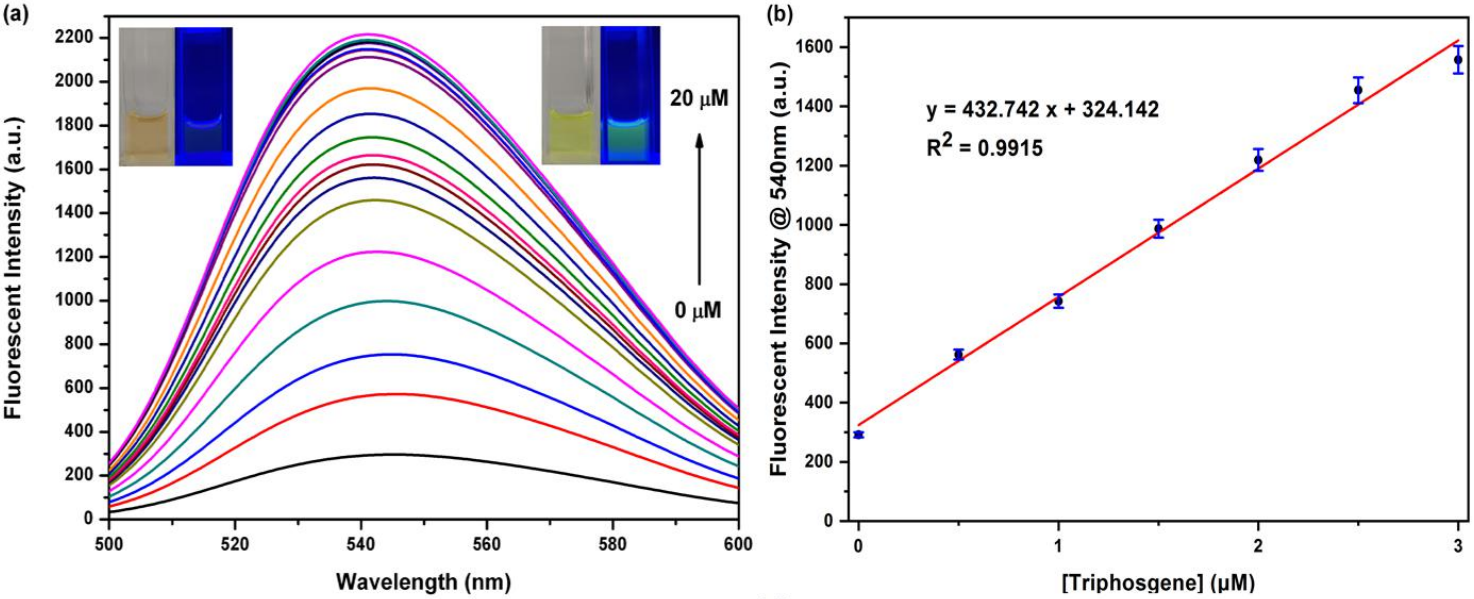

(c)

Blank Sample	F_{540}
1	291.9
2	296.1
3	299.6
4	300
5	299.8
6	301.2
7	301.6
8	291.1
9	301
10	292.7
σ	**3.95**

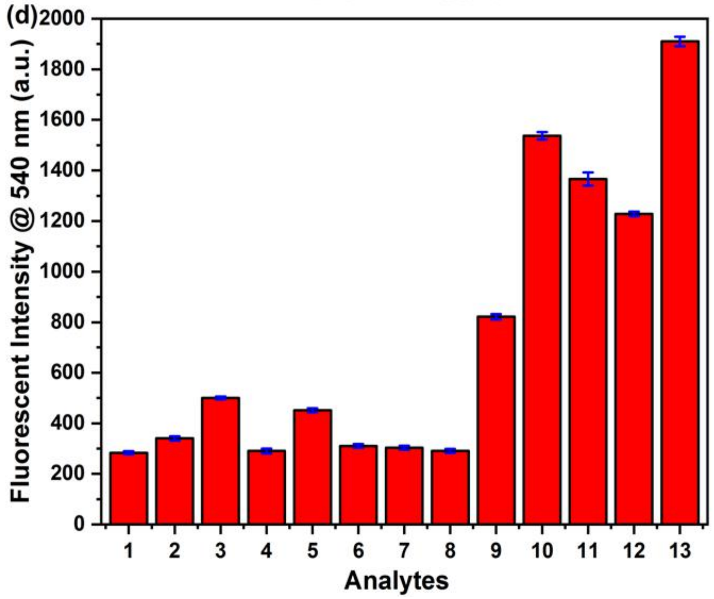

Fig. S17. (a) fluorescence spectra of Probe **3** (10 μM) in CH_3CN upon addition of an increasing amount of triphosgene (0−20 μM). (Inset) The color and fluorescence images of Probe **3** in the absence/ presence of triphosgene (λ_{ex} = 460 nm, slits: 10/10 nm). (b) The linear relationship between the fluorescence intensity at 540 nm and triphosgene concentration (0-3 μM) in CH_3CN; (c) Standard deviation (σ) of blank measurement from Fig. S17a; (d) fluorescent intensity at 540 nm of Probe **3** (10 μM) after the additions of analytes (30 μM) (1) Blank, (2) HCHO, (3) NO, (4) HCl, (5) $POCl_3$, (6) CH_3COCl, (7) $CH_2ClCOCl$, (8) $(COCl)_2$, (9) TsCl, (10) DCNP, (11) DCP, (12) $SOCl_2$, (13) Triphosgene (λ_{ex} = 460 nm, slits: 10/10 nm).

Table S2. Comparisons of several NBD-based fluorescent probes.

Probes	$\lambda_{ex}/\lambda_{em}$	Fluorescence	Detection Limit	Response time	Selectivity	References
NBD-OPD	λ_{ex}=270 nm λ_{em}=308 nm	Blue	0.7 ppb (2.3 nM)	2 min	Good	12
Probe 1	λ_{ex}=460 nm λ_{em}=525 nm	Green	1.2 nM	Within 20 s	Good	This work
Probe 2	λ_{ex}=460 nm λ_{em}=530 nm	Green	20.1 nM	Within 20 s	Poor	This work
Probe 3	λ_{ex}=460 nm λ_{em}=540 nm	Green	27.4 nM	Within 20 s	Poor	This work

References

1 W. Feng, S. Gong, E. Zhou, X. Yin, G. Feng, Readily prepared iminocoumarin for rapid, colorimetric and ratiometric fluorescent detection of phosgene, Anal. Chim. Acta, 2018, **1029**, 97-103.

2 S. L. Wang, L. Zhong, Q. H. Song, Sensitive and selective detection of phosgene, diphosgene, and triphosgene by a 3,4-diaminonaphthalimide in solutions and the gas phase, Chem.-Eur. J, 2018, **24**, 5652-5658.

3 M. Du, B. Huo, J. Liu, M. Li, A. Shen, X. Bai, et al., A turn-on fluorescent probe based on Si-rhodamine for sensitive and selective detection of phosgene in solution and in the gas phase, J. Mater. Chem. C, 2018, **6**, 10472-10479.

4 M. Sayar, E. Karakuş, T. Güner, B. Yildiz, U. H. Yildiz, M. Emrullahoğlu, A BODIPY-based

fluorescent probe to visually detect phosgene: toward the development of a handheld phosgene detector, Chem.-Eur. J, 2018, **24**, 3136-3140.

5 H. Xie, Y. Wu, F. Zeng, J. Chen, S. Wu, An AIE-based fluorescent test strip for the portable detection of gaseous phosgene, Chem. Commun, 2017, **53**, 9813-9816.

6 S. L. Wang, L. Zhong, Q. H. Song, A ratiometric fluorescent chemosensor for selective and visual detection of phosgene in solutions and in the gas phase, Chem. Commun, 2017, **53**, 1530-1533.

7 X. Wu, Z. Wu, Y. Yang, S. Han, A highly sensitive fluorogenic chemodosimeter for rapid visual detection of phosgene, Chem. Commun, 2012, **48**, 1895-1897.

8 H. Zhang, D. M. Rudkevich, A FRET approach to phosgene detection, Chem. Commun, 2007, **12**, 1238-1239.

9 X. Zhou, Y. Zeng, C. Liyan, X. Wu, J. Yoon, A fluorescent sensor for dual-channel discrimination between phosgene and a nerve-gas mimic, Angew. Chem.-Int. Edit, 2016, **55**, 4729-4733.

10 H. C. Xia, X. H. Xu, Q. H. Song, Fluorescent chemosensor for selective detection of phosgene in solutions and in gas phase, ACS Sens, 2017, **2**, 178-182.

11 Y. Zhang, A. Peng, X. Jie, Y. Lv, X. Wang, Z. Tian, A BODIPY-based fluorescent probe for detection of subnanomolar phosgene with rapid response and high selectivity, ACS Appl. Mater. Interfaces, 2017, **9**, 13920-13927.

12 Y. Hu, L. Chen, H. Jung, Y. Zeng, S. Lee, K.M.K. Swamy, et al., Effective strategy for colorimetric and fluorescence sensing of phosgene based on small organic dyes and nanofiber platforms, ACS Appl. Mater. Interfaces, 2016, **8**, 22246-22252.

13 T. I. Kim, B. Hwang, J. Bouffard, Y. Kim, Instantaneous colorimetric and fluorogenic

detection of phosgene with a meso-oxime-BODIPY, Anal. Chem, 2017, **89**, 12837-12842.

14 H. C. Xia, X. H. Xu, Q. H. Song, BODIPY-based fluorescent sensor for the recognization of phosgene in solutions and in gas phase, Anal. Chem, 2017, **89**, 4192-4197.

15 P. Kundu, K. C. Hwang, Rational design of fluorescent phosgene sensors, Anal. Chem, 2012, **84**, 4594-4597.

16 Q. Hu, C. Duan, J. Wu, D. Su, L. Zeng, R. Sheng, Colorimetric and ratiometric chemosensor for visual detection of gaseous phosgene based on anthracene carboxyimide membrane, Anal. Chem, 2018, **90**, 8686-8691.

17 Y. Hu, X. Zhou, H. Jung, S. J. Nam, M. H. Kim, J. Yoon, Colorimetric and fluorescent detecting phosgene by a second-generation chemosensor, Anal. Chem, 2018, **90**, 3382-3386.

18 L. Chen, D. Wu, J. M. Kim, J. Yoon, An ESIPT-based fluorescence probe for colorimetric, ratiometric, and selective detection of phosgene in solutions and the gas phase, Anal. Chem, 2017, **89**, 12596-12601.

19 W. Q. Zhang, K. Cheng, X. Yang, Q. Y. Li, H. Zhang, Z. Ma, et al., A benzothiadiazole-based fluorescent sensor for selective detection of oxalyl chloride and phosgene, Org. Chem. Front, 2017, **4**, 1719-1725.

20 T. I. Kim, D. Kim, J. Bouffard, Y. Kim, Rapid, specific, and ultrasensitive fluorogenic sensing of phosgene through an enhanced PeT mechanism, Sens. Actuator B-Chem, 2019, **283**, 458-462.

21 L. Bai, W. Feng, G. Feng, An ultrasensitive fluorescent probe for phosgene detection in solution and in air, Dyes Pigment, 2019, **163**, 483-488.

22 K. Maiti, D. Ghosh, R. Maiti, V. Vyas, P. Datta, D. Mandal, et al., Ratiometric chemodosimeter: an organic-nanofiber platform for sensing lethal phosgene gas, J. Mater.

Chem. A, 2019, **7**, 1756-1767.

23 P. Liu, N. Liu, C. Liu, Y. Jia, L. Huang, G. Zhou, et al., A colorimetric and ratiometric fluorescent probe with ultralow detection limit and high selectivity for phosgene sensing, Dyes Pigment, 2019, **163**, 489-495.

24 S. L. Wang, C. L. Zhang, Q. H. Song, Selectively instant-response nanofibers with a fluorescent chemosensor toward phosgene in gas phase, J. Mater. Chem. C, 2019, **7**, 1510-1517.

25 C. Wu, H. Xu, Y. Li, R. Xie, P. Li, X. Pang, et al., An ESIPT-based fluorescent probe for the detection of phosgene in the solution and gas phases, Talanta, 2019, **200**, 78-83.

26 S. L. Wang, C. Li, Q. H. Song, Fluorescent chemosensor for dual-channel discrimination between phosgene and triphosgene, Anal Chem, 2019, **91**, 5690-5697.